Journal of the Meteorological Society of Japan, Vol. 74, No. 2, pp. 155–166, 1996

Tropical Deep Convection, Convective Available Potential Energy and Sea Surface Temperature

By G.S. Bhat, J. Srinivasan[1] and Sulochana Gadgil

Centre for Atmospheric Sciences, Indian Institute of Science, Bangalore 560 012, India

(Manuscript received 26 December 1994, in revised form 25 December 1995)

Abstract

The convective available potential energy (CAPE) based on monthly mean sounding has been shown to be relevant to deep convection in the tropics. The variation of CAPE with SST has been found to be similar to the variation of the frequency of deep convection at one station each in the tropical Atlantic and W. Pacific oceans. This suggests a strong link between the frequency of tropical convection and CAPE. It has been shown that CAPE so derived can be interpreted as the work potential of the atmosphere above the boundary layer with ascent in the convective region and subsidence in the surrounding cloud-free region.

1. Introduction

An important aspect of the ocean-atmosphere interaction over the tropical oceans is the relationship between the sea surface temperature (SST) and organized deep convection (henceforth tropical convection) in the atmosphere. It was recognized almost five decades ago by Palmen (1948) that SST has to be above a certain value for intensification of the tropical disturbances to the cyclone stage. In a seminal paper, Bjerknes (1969) showed that the variation of convection over the tropical Pacific could be attributed to the variations of SST. Systematic investigation of the variation of convection and its relationship with SST became possible only after the availability of satellite data. Studies of the variation of tropical convection over oceans with SST based on different measures of organized deep convection such as cloudiness intensity (Gadgil *et al.*, 1984), outgoing longwave radiation (OLR) (Graham and Barnett 1987, Zhang 1993), and the frequency of highly reflective clouds (HRC) (Waliser *et al.*, 1993) all suggest a similar and highly non-linear relationship.

Consider, for example, the variation with SST of the average number of convective days per month (inferred from the frequency of occurrence of highly reflective clouds in the visible satellite mosaics, see *e.g.*, Garcia 1985) over tropical oceans shown in Fig. 1a (adapted from Waliser *et al.*, 1993). The nature of the variation is rather similar over different regions. An idealized representation of the important features of this variation is shown schematically in Fig. 1b. When the SST is below a temperature T_o (henceforth the Palmen threshold), no organized deep convection occurs. Above the Palmen threshold (i) first there is a slow increase of the frequency of tropical convection with SST followed by (ii) a sharp increase with SST over a range of 1–2°C and (iii) very small changes for higher values of SST. The range of SST over which there is a rapid change in convection [(ii) above] will henceforth be called the critical range. Note that the slopes of the mean HRC curve with SST in the critical range are similar in different regions. The critical SST range varies, however, from region to region, being around 27–29°C for the Pacific and 26.5–27.5°C for the Atlantic. There are other regional differences as well. For example, the phase of slow increase with SST is not seen in the W Pacific.

The Palmen threshold corresponds to the minimum SST at which the tropical atmosphere becomes vertically unstable, and deep convection can be triggered (*e.g.*, Palmen 1948). The reasons for the observed behaviour of tropical convection for SSTs larger than T_o have not been elucidated so far. The saturation water vapour mixing ratio q_s is a highly non-linear function of the temperature and hence could play an important role. Lau and Shen (1988) and, Neelin and Held (1987), suggest, however, that this non-linearity is not sufficient to explain the non-linear variation of the tropical convection with SST. Therefore the relationship between SST and tropical deep convection is yet to be satisfactorily explained.

1 also at Jawaharlal Nehru Centre for Advanced Scientific Research, Bangalore, India

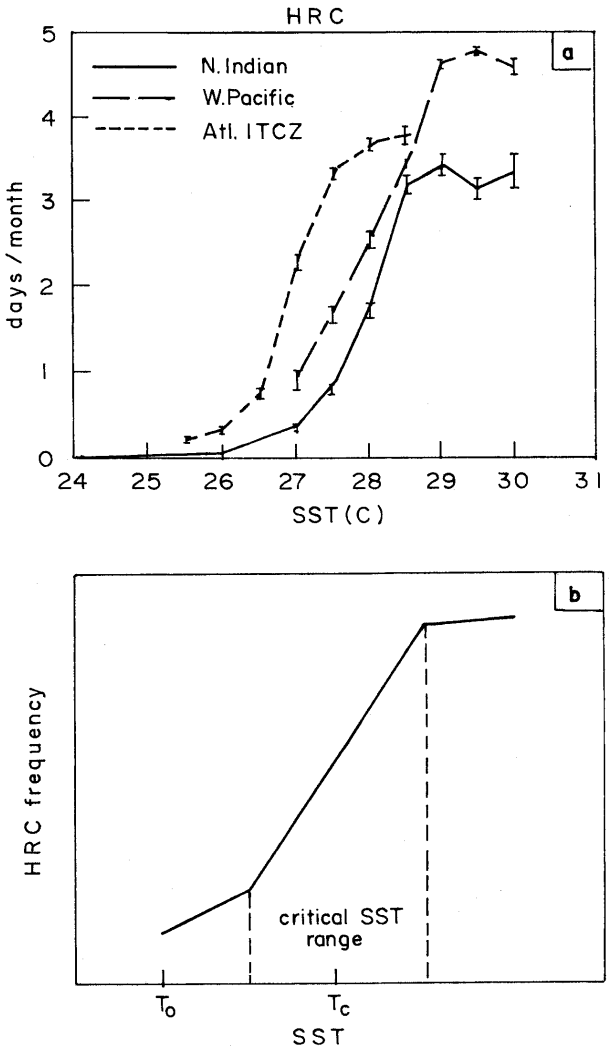

Fig. 1. (a) Variation of Mean HRC with SST over tropical oceans. The regions are, North Indian ocean — 60–106°E 10–15°N; W. Pacific — 120–150°E 10°S–10°N; Atlantic — 15–45°W 4–12°N. Error bars denote standard error of the means for each SST bin. (Adapted from Waliser *et al.*, 1993.) (b) A schematic of the variation of mean HRC with SST.

In this paper, an attempt is made to gain insight into this observed variation of tropical deep convection.

We note that while the mean values of the various measures of intensity of convection (such as OLR or HRC) exhibit the pattern of variation with SST observed in Fig. 1, there is a significant scatter about the mean (*e.g.*, Zhang 1993). This is not surprising, since tropical convection is known to depend on factors such as the large-scale convergence and divergence (Graham and Barnett 1987, Neelin and Held 1987, Fu *et al.*, 1994), and convective inhibition energy (CINE, Willaims and Renno 1993), in addition to its well-known dependence on SST. Here, we restrict our attention to the variation of the mean tropical convection with SST.

Tropical deep convection is governed by both local and large-scale influences. By local influence, we mean the influence of the thermodynamic properties of the surface or the mixed-layer air[1], which are important since they influence the energy/entropy of the cloud air. These properties are strongly influenced by the local SST (*e.g.*, Betts and Ridgway 1989). The upper air[2] is directly coupled to the mixed-layer air only in regions of deep convection. Over most of the regions (and on most of the days) the tropical belt is characterized by large-scale subsidence and radiative cooling, *i.e.*, radiative-convective equilibrium (Emanuel 1994). The subsiding air originates from the outflow of deep convective systems existing elsewhere in the tropics. Hence, the thermodynamic properties of the upper air are not necessarily related to the local surface conditions.

A positive cloud buoyancy over a large depth of the atmosphere is required for maintaining deep convection in the tropics. The buoyancy of the cloud depends on the properties of the mixed-layer air and that of the upper air through which it rises. Hence we expect a parameter that includes the effect of the properties of the surface layer and the upper air to be better correlated with deep convection than one based on surface properties alone. We have investigated here one such parameter — the convective available potential energy (CAPE), because of its special features viz.,

a) CAPE is zero below a certain SST, as is the case with deep convection,

b) CAPE is a measure of the instability in the atmosphere under moist convection, and a positive CAPE is necessary for the occurrence of deep convection, and

c) CAPE has been shown to play an important role in systems ranging in scale from thunderstorms (Williams *et al.*, 1992) through mesoscale systems (Moncrief and Miller 1976).

We have used monthly mean soundings for estimating CAPE, since we are concerned with the variation of tropical convection on a monthly/seasonal scale. In Section 2 we discuss the method of calculation of CAPE. We indicate the data sources used for the present study in Section 3. In Section 4, we show that the variation of CAPE with SST is similar to that of the variation of HRC with SST in the West Pacific and Atlantic oceans. In Section 5 we show that CAPE based on a mean sounding can be interpreted as the potential for work production in

1 In this study, the surface layer, the mixed layer, the subcloud layer, and the boundary layer, are all taken to mean the lowest 0.5 km or so of the atmosphere above the ocean, and no specific distinction is made among them.

2 We refer to the entire troposphere above the subcloud layer as upper air.

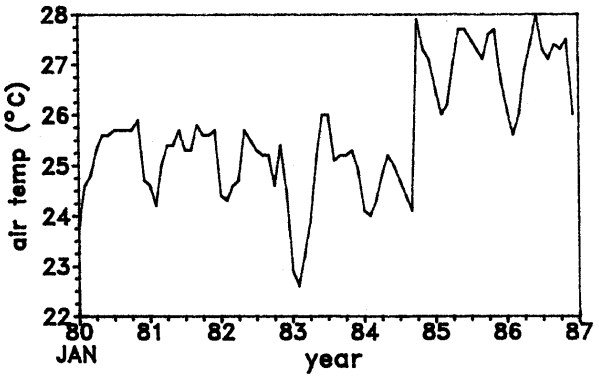

Fig. 2. Time series of surface air temperature from the Monthly Climatic Data of the World for Guam.

the atmosphere above the subcloud layer comprising of ascent in the convective zone and descent in the surrounding cloud-free region.

2. Estimation of cape

CAPE is the work done by the buoyancy force on a parcel on ascent under moist convection, and can be calculated from the integral (*e.g.*, Williams and Renno 1993),

$$\text{CAPE} = \int_{\text{LFC}}^{\text{LNB}} (T_{vp} - T_{ve}) R_d \, d(\ln p), \qquad (1)$$

where T_{vp} and T_{ve} are the virtual temperatures of the parcel and the environment respectively, R_d is the gas constant of dry air and p is pressure. (The virtual temperature T_v of moist air is given by the expression $T_v = T(1 + 0.608\ q_v - q_l)$, where T is the air temperature, q_v and q_l are water vapour and condensed water mixing ratio, respectively.) LFC (level of free convection), and LNB (level of neutral buoyancy, also known as the level of vanishing buoyancy LVB) are respectively lower and upper limits between which the parcel buoyancy is positive.

Condensation, precipitation, freezing of liquid water, and the level of parcel origin, all influence the virtual temperature of the air parcel and hence CAPE as the parcel undergoes undiluted ascent in the atmosphere (*e.g.*, Saunders 1957, Emanuel 1994, Fu *et al.*, 1994). Xu and Emanuel (1989) pointed out that the estimated buoyancy for tropical soundings, even for undiluted ascent, is within the uncertainties in measurements when all the condensed water is retained in the cloud, (*i.e.*, for the reversible moist adiabatic process). This is valid for real clouds if the reversible moist adiabatic process is the relevant reference moist process in the atmosphere. However, it has been shown that for a deep cloud in which glaciation takes place, the estimated CAPE is almost independent of the cloud microphysical details, and a pseudoadiabatic process can be used to calculate parcel properties for the purpose of estimating CAPE (Williams and Renno 1993). Further, Fu *et al.*, (1994) have shown that the observed cloud tops are more consistent with a pseudoadiabatic limit rather than a reversible moist adiabatic limit, and that for this process CAPE is much larger than the uncertainties involved due to the measurement errors. Hence in this study CAPE is calculated assuming the pseudoadiabatic process.

3. Data

The present study is concerned with the variation of tropical convection on a monthly/seasonal scale, and hence uses monthly mean soundings for estimating CAPE. This will be denoted by MCAPE in order to distinguish it from CAPE based on an individual (*i.e.*, daily) sounding. In Appendix A the relationship between daily CAPE and MCAPE is considered and it is shown that MCAPE is comparable to monthly averages of daily CAPE.

The soundings published in the Monthly Climatic Data of the World (Ashville) have been used here. These represent an average of the soundings taken during convective as well as non-convective periods in each month, and can be thought of as representing the average thermal structure of the atmosphere in the region. The SST data analyzed are from COADS (Slutz *et al.*, 1985), given as averages for each 2° × 2° (latitude-longitude) grid area. These data are considered to be reliable when the frequency of observation in the grid is large (Trenberth *et al.*, 1992). So island stations, where regular soundings are available, and COADS data shows a sufficiently large frequency of ship observations in the grid box where the sounding station is located, are considered appropriate for the present purpose. Figure 1a shows that Atlantic and Pacific oceans have clearly distinct critical SST ranges. Therefore, we consider one station each from these oceans viz. the islands of Guam (13°28′N, 144°47′E) and Grantley Adams AP (13°04′N, 59°29′W). The COADS data show relatively large number of observations for each month in the respective grids. The statistics for the period 1974–83 showed that the mean number of observations per month for Guam is 39 with a standard deviation of 13, and that for Grantley is 18 with a standard deviation of 6.

Figure 2 shows the surface air temperature reported in the soundings for Guam. The sudden jump in the surface air temperature from 1985 is a result of change in the observation time from 1200 GMT prior to 1985 to 0000 GMT thereafter. The difference in the average temperature corresponding to these two reporting times is about 2°C, reflecting the strong contribution from the diurnal cycle. Therefore, the surface air temperature measured at the island station depends on the observation time during the day, and cannot be taken to

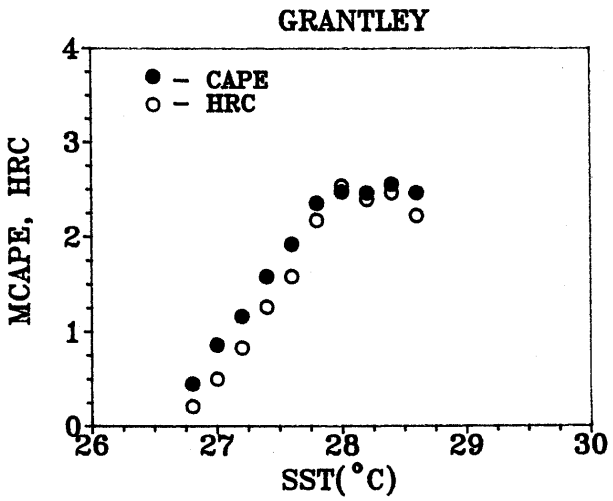

Fig. 3. Variation of mean MCAPE (kJ/kg) and HRC (days/month) with SST for Grantley Adams AP, assuming an air-sea temperature difference of −1°C. The data period is January 1979–December 1986.

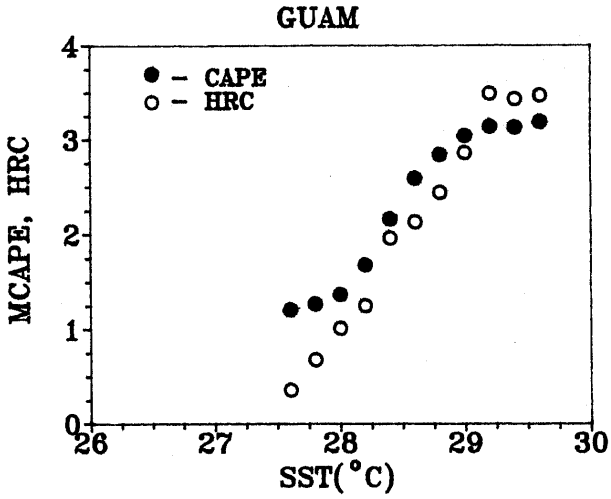

Fig. 4. Variation of mean MCAPE (kJ/kg) and HRC (days/month) with SST for Guam assuming an air-sea temperature difference of −1°C. The data period is January 1979–December 1986.

represent the air temperature over the ocean, which is likely to show a smaller diurnal component (*e.g.*, LeMone 1980). In Appendix B, it is shown that COADS surface air temperature is also not accurate at these two grids. Hence, the surface air temperature in the present study is obtained from SST by assuming an air-sea temperature difference ranging between −0.5° and −1.5°C, a typical range given in the Atlas by Bottomley *et al.* (1990). Computations showed that the main conclusions of this paper are not dependent on the actual temperature difference assumed, provided it is in the range reported by Bottomly *et al.* (1990). Unlike the air temperature, water vapour content is not likely to be affected by land-sea contrast for a tiny island station. Therefore, the humidity value given in the sounding data is taken to be representative of the surrounding oceanic region.

As mentioned in the introduction, OLR and HRC have been used to infer the index of deep convection. A monthly mean value for OLR below 240 W/M^2 is generally taken to imply the presence of large-scale deep convection. The HRC data are a little more subjective, and have been prepared by simultaneously looking at visible and infrared satellite mosaics, filtering out the low- and mid-level highly reflective clouds (Garcia 1985). Waliser *et al.* (1993) compared OLR and HRC and conclude that HRC is a reliable index of deep convection. Further, compared to OLR, HRC has one major advantage, that is, in the absence of deep convection, its value is zero. For these reasons, HRC is taken as the proxy for deep convection in this study. The HRC values shown henceforth are averages for the 2° × 2° grid area, which corresponds to the COADS SST grid area.

4. Results

MCAPE has been calculated for the monthly mean soundings for the period 1979 to 1986, assuming a moist pseudoadiabatic ascent of the surface air. A moving window with a width of 0.5°C is employed and the average for the window has been calculated at SST intervals of 0.2°C. The results for Grantley are shown in Fig. 3, and that for Guam in Fig. 4. In these figures, a result is shown only if the number of samples within the window is at least 10. It is seen that in the 26.5°C to 28.5°C SST range, the variations of HRC and MCAPE with SST are similar for Grantley. For Guam, the trends are similar in the 28°C to 29.5°C SST range; however, in between 27.5°C to 28°C and at 29°C SST the agreement is not very good. Varying the sea-air temperature difference by ±0.5°C about the value of 1°C assumed in Figs. 3 and 4 shifts MCAPE by ±0.15 kJ/kg throughout. Thus the results do not depend on the exact air-sea temperature difference assumed, provided it is in the range observed over tropics.

It is seen from Figs. 3 and 4 that the variation of MCAPE is rather similar to that of HRC. This suggests a strong relationship between HRC and MCAPE. A scatter plot based on combined data for the two regions shows that MCAPE and HRC are highly correlated (Fig. 5). The Pearson product moment correlation coefficient is 0.93 which is significant at the 1 % level. Note that the fit of the linear regression is remarkably good. Thus although the

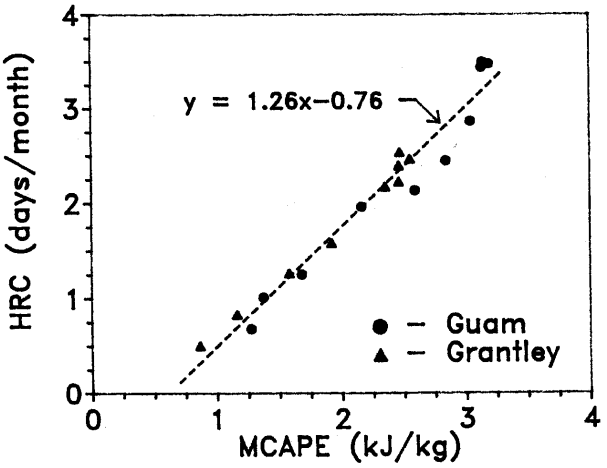

Fig. 5. Scatter plot of HRC versus MCAPE. Values of HRC $\geq$ 0.5 day/month are only shown.

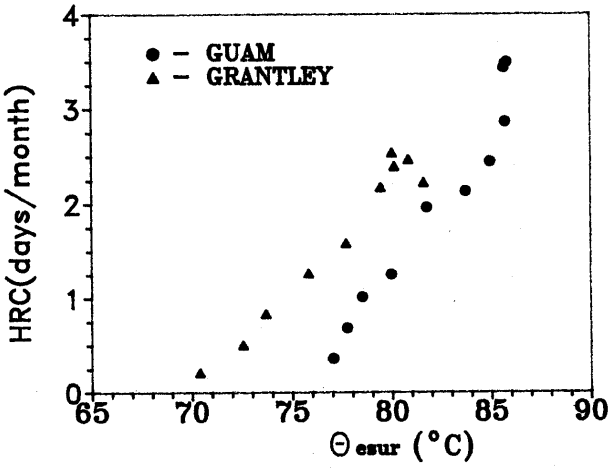

Fig. 6. Scatter plot of HRC versus θ_{esur}.

relationship between convection and SST is highly non-linear, that between convection and MCAPE appears to be linear.

With the data available to us, we looked for other tropical small island stations, for which regular soundings up to the tropopause and with a reasonable frequency of SST observations are available. In the Indian ocean, Minicoy is the only station that has good SST coverage. The upper air soundings are, however, missing in this station on about 35 % of the months. In the Pacific, stations like Koror, Majuro, Truk, Tarawa, Funafuti, *etc.* have good sounding data but the frequency of SST observations is very poor (the average number of observations per month is not more than 5 and often around 2). The equatorial Atlantic is no better. Therefore, in the present study, the analysis is restricted to Gaum and Grantley.

We note that in the expression (1) for MCAPE, T_{ve} is related to the thermal structure of the troposphere which results from radiative — convective equilibrium of the atmosphere (Emanuel 1994). On the other hand, T_{vp}, related to the surface layer air properties, is determined by the large-scale circulation and SST (Betts and Ridgway 1989, Emanuel 1994). Therefore, MCAPE, though basically a thermodynamic parameter, incorporates the effects of most of the large-scale circulation processes.

The question then arises as to whether it is necessary to incorporate the effects of the upper air or can the variation of tropical convection be understood in terms of the variation of surface air properties alone? For tropical convection, perhaps the most relevant attribute of the surface air is its equivalent potential temperature (θ_{esur}). The equivalent potential temperature represents the total energy as well as the entropy of the moist air and deep convection is favoured when θ_{esur} is above a threshold (Betts and Ridgeway 1989). The variation of HRC with θ_{esur} for Guam and Gantley is shown in Fig. 6. It is seen that for each region there is a range over which HRC increases linearly with θ_{esur}. However, note that unlike the case of MCAPE (Fig. 5), the curves for the two regions are distinct. This could be because θ_{esur} represents only the surface component of deep convection and does not incorporate the regional differences in the upper air properties.

What Figs. 3–6 clearly demonstrate is that the mean HRC points collapse better when plotted against MCAPE than against surface thermodynamic parameters. It cannot be a mere coincidence that data for two grids, one located near the warm pool of the Western Pacific and the other in the Atlantic ocean (chosen because of good quality data) fall along a line. In our view, MCAPE is a better thermodynamic parameter to correlate with HRC than others considered so far. The possibility that the slope of HRC-versus-MCAPE curve may differ over other locations is not ruled out by the present study.

Next we offer a physical interpretation of MCAPE.

5. Interpretation of cape based on a mean sounding

CAPE based on an individual sounding is the work done by the buoyancy force acting on the parcel under moist adiabatic ascent in the atmosphere. The same meaning can not be ascribed to CAPE based on a monthly mean sounding, and its physical meaning needs to be established. We provide a new interpretation of MCAPE in this section.

Note that in the tropical atmosphere on any given day, there are relatively narrow regions of ascent with deep moist convection surrounded by a larger region of descent under cloud-free or shallow cloud

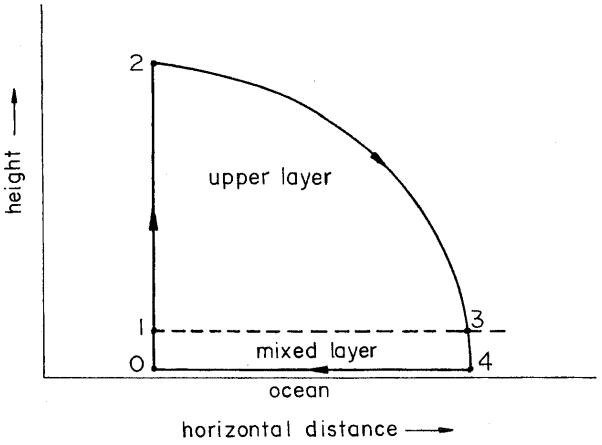

Fig. 7. A schematic of the path of air associated with deep convection and large-scale circulation in tropics.

conditions. The number of days of convection at any point in space is usually much smaller than those without any convection (average number of convective days is generally not more than about 4 days/month, Fig. 1a). Therefore, an average sounding for a large-scale area or for a long period such as a month, represents the average thermal structure containing convective and cloud-free regions/periods, with greater weighting for the latter.

5.1 The model

For interpreting MCAPE, we find it convenient to think of the atmospheric circulation as a natural heat engine, with air ascending in the convective region and subsiding in the surrounding clear area (see Appendix C). The region of ascent in which the moist air converges at low levels and ascends in cumulonimbus clouds, and diverges at high levels (150 to 300 mb), is an important component of the engine. Most of the water vapour initially contained in the air is condensed out in the process. Though air in the atmosphere does not follow a closed cycle, it is convenient to imagine that the air parcel is enclosed in a highly flexible and heat conducting balloon such that pressure and temperature (and also density) inside and outside the balloon are equal. In many engineering applications where the air does not follow a closed cycle (the automobile engine for example), assumption of an equivalent closed cycle and its analysis provides a useful approximation to the performance of the real engine (Heywood 1988). In this spirit, Fig. 7 shows a schematic of the path followed by an air parcel associated with the synoptic and large-scale circulation system in the tropics. The path comprises the ascending (1-2), subsiding (2-3) and mixed or subcloud layer branches (3-4-0-1). The ascending branch is supposed to represent the average condition in the convective region. The subsidence branch is the average state of the atmosphere in the clear region sufficiently away but surrounding the convective area. The lower end of ascending and subsiding branches (Points 1 and 3, respectively) is the top of the atmospheric mixed-layer, and the upper end (Point 2) is the level where the virtual temperatures of the two branches are equal. Points 4 and 0 are next to the sea surface in the subsiding and convective regions, respectively.

For a unit mass of air that takes part in this process, the work done during a complete cycle is given by,

$$W = \oint p\, dv, \tag{2}$$

where v is the specific volume. For the present cycle, it is convenient to split W into two parts, W_{tr}, the work done in the troposphere above the cloud base which is mainly due to moist convection (Path 1-2-3), and W_{sl}, the work done in the surface layer (Path 3-4-0-1), *i.e.*,

$$W = W_{tr} + W_{sl} = \int_1^3 p\, dv + \int_3^1 p\, dv. \tag{3}$$

Using the ideal gas law for moist air in the form $pv = R_d T_v$, W_{sl} can be expressed as,

$$W_{sl} = R_d(T_{v1} - T_{v3}) - R_d \left[\int_3^4 T_v d(\ln p) + \int_4^0 T_v d(\ln p) + \int_0^1 T_v d(\ln p)\right]. \tag{4}$$

Within the mixed-layer, the virtual potential temperature θ_v [$= (1000/p)^{\kappa}$] is approximately constant in the vertical, and using this (4) can be integrated to give,

$$W_{sl} = R_d(T_{v1} - T_{v3}) - R_d[(T_{v4} + T_{v1} - T_{v3} - T_{v0})/\kappa + T_{vm} \ln(p_0/p_4)], \tag{5}$$

where T_{vm} is the mean virtual temperature of the air along Path 4-0. The last term represents the integral along the surface (*i.e.*, 4 to 0). Assuming that the virtual temperature is a linear function of surface pressure, it can be shown that the integral is $[\ln(p_0/p_4)\ (T_{vm} + dT_v/dp_s(p_4 - p_{sm})]$, where p_s is the surface pressure and p_{sm} is the mean surface pressure along 4 to 0. Since $(T_{v1} - T_{v4}) \ll T_{vm}$, the contribution of terms other than T_{vm} can be neglected in this integral. For conditions that prevail over tropical oceans, $p_4 \approx 1000$ to 1010 mb, Δp_s $(= p_4 - p_0)$ is 5 to 30 mb for convective systems that occur most of the time, and T_{vm} is about 29°C. The height of the mixed-layer Δp_m [$= (p_0 - p_1)$ or $(p_4 - p_3)$] is about 50 mb over tropical oceans (LeMone 1980). Corresponding to these values, W_{sl} is well approximated by

$$\begin{aligned} W_{sl} &= R_d(T_{v1} - T_{v3}) \\ &\quad - R_d[(\Delta p_m/p_0)(T_{v4} - T_{v0}) + T_{vm} \ln(p_0/p_4)] \\ &\approx R_d(T_{v1} - T_{v3}) + R_d T_{vm} \Delta p_s/p_4. \end{aligned} \tag{6}$$

Next, consider the work done in the troposphere above the cloud base, W_{tr}, which can be expressed as,

$$W_{tr} = \int_1^2 R_d T_{va} d(\ln p) + \int_2^3 R_d T_{vs} d(\ln p) + R_d(T_{v3} - T_{v1}), \quad (7)$$

where T_{va} and T_{vs} are virtual temperatures in the ascending and subsiding branches, respectively. Under the assumption $p_1 = p_3$, (7) reduces to,

$$W_{tr} = \int_1^2 R_d(T_{va} - T_{vs}) d(\ln p) + R_d(T_{v3} - T_{v1}). \quad (8)$$

The first term on the right-hand side of (8) can be expressed as

$$R_d \int_1^2 (T_{vp} - T_{ve}) d(\ln p) + R_d \int_1^2 (T_{ve} - T_{vs}) d(\ln p) - R_d \int_1^2 (T_{vp} - T_{va}) d(\ln p), \quad (9)$$

where T_{vp} is the virtual temperature of the air parcel ascending moist adiabatically from the surface layer and T_{ve} is the regional monthly mean virtual temperature. The first term on the right-hand side of (9) is MCAPE. Consider the second term. The area occupied by the convectively active region is usually very small compared to the area of subsidence. As a result, the average sounding is dominated by that of the subsiding clear region, and T_{vs} can be considered to be equal to the regional monthly mean sounding T_{ve} for all practical purposes. Therefore, the second integral can be taken to be small, if not zero. Since T_{va} is the virtual temperature of the atmosphere in the ascending (*i.e.*, deep convective) region, by definition, the last integral is the convective available potential energy in the ascending region (denoted by ACAPE). Note that ACAPE represents the convective instability of the atmosphere in the ascending area, whereas, MCAPE represents the average convective instability of the atmosphere in the region comprising the ascending and subsiding areas. Therefore (8) can be written as

$$W_{tr} = \text{MCAPE} - \text{ACAPE} + R_d(T_{v3} - T_{v1}). \quad (10)$$

The last term on the right-hand side of (10) is the contribution from the surface temperature gradient. In the present model, the subsiding branch is assumed to be in the clear region surrounding the convective area, and hence T_{v1} and T_{v3} may differ by 1° to 2°C at most. Then the contribution of the last term (about 0.5 kJ/kg) is smaller than a typical value of MCAPE (which is about 2–3 kJ/kg, Figs. 3 and 4).

The total work done during a complete cycle is obtained by adding (6) and (10), *i.e.*,

$$W = R_d T_{vm} \Delta p_s / p_4 + \text{MCAPE} - \text{ACAPE} \quad (11)$$

We shall call the first term as the contribution of the surface pressure gradient and the remaining two terms as the contribution of the deep convection to the total work. Notice that even in the absence of horizontal temperature and pressure gradients, the work produced during a cycle could be positive. We focus on the contribution of deep convection to the net work next.

5.2 Limiting cases

Let us consider a few limiting cases of the the contribution of the deep convection.

(a) Suppose that the surface air ascends in cumulonimbus clouds moist adiabatically without modifying its surrounding environment. Therefore, $T_{va} = T_{ve}$, MCAPE and ACAPE are equal and deep convection does not contribute to W_{tr}. In such a situation, the work done by the buoyancy force on the cloud air increases the vertical velocity w in the cloud. Due to the large vertical velocity that could result ($w \sim \sqrt{2\text{ACAPE}}$), the cloud air will rise far above its level of neutral buoyancy, and its kinetic energy will decay in the stratosphere after a few damped oscillations (Ebert and Holland 1992). Therefore, all the energy released by the moist convection is dissipated in the stratosphere, with no contribution to the large-scale circulation in the troposphere.

(b) The atmosphere in the convective area becomes moist neutral, *i.e.*, the entire troposphere approaches the moist pseudoadiabatic temperature structure. Then, $T_{va} = T_{vp}$, ACAPE = 0, and W = MCAPE.

Notice that no buoyancy force will act on the cloud air as such, and so its vertical velocity will not increase above cloud base. At any given height (pressure) in the troposphere, the ascending air is warmer than the subsiding air, and this expansion at warmer and compression at colder temperatures results in net work being produced in the large-scale system as air moves from 1 to 3. This work can be used for maintaining the large-scale circulation, such as to overcome the frictional dissipation. Whereas in the previous case, the energy released gets dissipated in the stratosphere, in this case, it can contribute to the maintenance of the circulation associated with the organized convection.

(c) The ascending cloud air is diluted by the entrainment of dry environmental air such that its buoyancy is nearly zero. This process is no longer adiabatic, and Eq. (10) is not applicable in the strict sense. However, interpreting ACAPE as the integral of the buoyancy force acting on the real cloud air in the area of ascent, allows the extension of (10) to this case also. From this assumption, ACAPE ≈ 0. The work, W_{tr}, depends on the thermal structure of the atmosphere in the ascending region (see Eq. (8)). Since cloud mass flux increases with height

due to entrainment, subsidence is induced in the immediate surroundings to satisfy mass conservation, causing warming of the atmosphere in the convective area (Arakawa and Schubert 1974). Hence T_{va} could be larger than T_{ve} and W_{tr} can be positive. It is important to note that, the more stable the atmosphere, the larger is W_{tr}. However, the atmosphere may not approach the moist adiabatic lapse rate (which is the extreme value), and W_{tr} in this case will in general be smaller than that compared to Case (b).

5.3 Observed behaviour of tropical convective systems

Consider the observed behaviour of tropical convective systems. There is strong observational evidence that regions of deep convection in the tropics are more stable. The warming of the troposphere in tropical cyclones and hurricanes has been recognized for a long time (Frank 1977). The atmosphere becomes stable even in the weaker convective systems such as those associated with mesoscale events embedded in the ITCZ. Betts (1986) showed that the atmosphere approaches a state which is slightly unstable to a reversible moist adiabat of low-level air a few hundred millibars above cloud base, and a pseudoadiabat of low-level air above the freezing level in deep convective systems in the tropics. Emanuel *et al.* (1994) argue that the virtual temperature of the convecting atmosphere in the tropics is uniquely related to the mixed-layer entropy, and the atmosphere in these regions is almost moist neutral. All these studies suggest that ACAPE is small, and observations indicate that ACAPE is in general less than 1000 J/kg (Emanuel *et al.*, 1994).

Next, consider the role of entrainment in deep clouds, which as we have seen in Section 5.2 can reduce W_{tr}. The lateral entrainment of ambient air into cumulonimbus clouds is an important but poorly understood process. In non-precipitating clouds, there is sufficient observational evidence that air within these clouds rises without much lateral mixing (Paluch 1979, Emanuel 1994, pp. 199–206). There is little reason to believe that the entrainment process should be different in cumulus and cumulonimbus clouds during the cloud growth stage. Further, Fu *et al.* (1994) note that cloud-top heights observed in the tropics are consistent with a pseudoadiabatic limit, suggesting that, overall, a pseudoadiabatic process better approximates the thermodynamic process in deep clouds in the tropics. Hence, there is not sufficient grounds to believe that lateral entrainment significantly influences the development of deep clouds. Therefore, conditions in the tropical atmosphere seem to be in between the limiting cases (a) and (b) discussed in Section 5.2, with MCAPE at least two to three times larger than ACAPE during convective months. Thus MCAPE is larger than ACAPE in the tropics, and expected to dominate W_{tr}. Hence interpretation of MCAPE as the work potential of the troposphere seems appropriate.

6. Discussion

The present work sheds new light on the role of moist convection in tropical dynamics and energetics. Perceptions of tropical convection have undergone major changes during the last forty years. Charney and Eliassen (1964) proposed that hurricane depression (a form of tropical deep convection) and cumulus clouds support one another — the cumulus cell by supplying the heat energy for driving the depression, and the depression by producing the low-level convergence of moisture into the cumulus cell. In this theory, the moist convection is an energetically important component of tropical disturbances. The recent ideas oppose the Charney and Eliassen's theory and propose that "tropical deep convection is a response to instability produced by large-scale processes" (Emanuel 1994, Emanuel *et al.*, 1994). In this scenario, processes that enhance instability are responsible for maintaining the tropical circulation. Since moist convection reduces the instability of the atmosphere, it is considered to be a drag on the tropical circulation. Note that in all these arguments, the stress is on the convecting region only.

The analysis presented in Section 5.2 shows that, for assessing the role of moist convection in the tropics, the ascending region should not be considered in isolation. We have shown that the work done in the large-scale system by moist convection is maximum when the ascending region is moist neutral. Hence we can argue that the prefered state of the atmosphere in the ascending region is moist neutral because it maximizes the work produced in the system. Therefore, moist convection can be an energetically important component of tropical circulation despite the convecting region being moist neutral.

The important result of the present work is that tropical convection is related to MCAPE, the average convective instability of the atmosphere in the region as a whole. This idea is not inconsistent with the thinking that the large-scale processes, like mixed-layer dynamics and radiative-convective equilibrium, that enhance the instability of the atmosphere are important factors in tropical circulation (Emanuel *et al.*, 1994). These processes enhance MCAPE also by increasing T_{vp} and decreasing T_{ve}, (see Eq. (1)), and hence the convective activity in the region. The convective activity itself could have a negative effect on MCAPE. When the frequency of convection increases, the associated mesoscale downdraughts and their effect on the ocean has a tendency to decrease the energy (entropy) of the subcloud layer air (Emanuel *et al.*, 1994). The upper

atmosphere begins to feel the local surface conditions more often, linking T_{vp} and T_{ve} directly. Both these processes tend to decrease the instability of the atmosphere, and hence MCAPE.

In the present work, the analysis has been restricted to variations in MCAPE and HRC associated with variations in SSTs over two representative stations with adequate data. Further studies are required to test the linear relationship between MCAPE and HRC for other regions as well, using good quality data that represent the average thermal conditions in these regions. If the above relationship between MCAPE and deep convection is indeed found to be valid for the entire tropical belt, it will have far-reaching implications. Then it may become possible to understand space-time variations of convection in terms of the variation of surface properties and the atmospheric profiles which in turn are determined by the tropical circulation, and the location and intensity of the Hadley and Walker cells *etc.*

7. Conclusions

We have shown that the frequency of tropical convection correlates linearly with MCAPE with a correlation coefficient of 0.93, when the data are combined for one station each from the Pacific and Atlantic oceans. We have demonstrated that the frequency of tropical convection is better correlated with MCAPE than with θ_{esur}, which depends on surface air properties alone. This suggests that MCAPE, which depends upon the surface and upper air thermodynamic properties, is an important quantity to link deep convection with SST over the tropical oceans. We have also provided a physical interpretation for MCAPE. It is shown that MCAPE can be thought of as the work potential of the atmosphere above the subcloud layer with ascent in the convective region and subsidence in the surrounding cloud-free region.

Acknowledgments

This work was sponsored by a grant from the Department of Ocean Development, New Delhi, India. The authors also thank the two referees whose critical comments have improved the paper.

Appendix

A : MCAPE and the Average of Daily CAPE

In the expression for CAPE (Eq. 1), T_{vp}, the cloud-parcel virtual temperature, is uniquely related to the surface wet-bulb potential temperature θ_{ws} and pressure for a pseudoadiabatic process. Therefore, we can express T_{vp} as,

$$T_{vp} = f(\theta_{ws}, p). \tag{A1}$$

Using the Taylor expansion about the wet-bulb potential temperature $\overline{\theta}_{ws}$ based on monthly mean temperature and humidity, (A1) can be expressed as

$$\begin{aligned} T_{vp} &= f(\overline{\theta}_{ws}, p) + k(p)(\theta_{ws} - \overline{\theta}_{ws}) \\ &\quad + \text{higher order terms} \\ &= \overline{T}_{vp} + k(p)(\theta_{ws} - \overline{\theta}_{ws}) \\ &\quad + \text{higher order terms}, \end{aligned} \tag{A2}$$

where, $k(p) = (\partial f/\partial\theta_w)\,|_{\theta_w=\overline{\theta}_{ws}}$. On a $T-\phi$ diagram, the moist adiabats are parallel for a variation in θ_{ws} of about +3°C, a typical range observed over tropical oceans (*e.g.*, Williams and Renno 1993). Hence, the higher-order terms are negligible in (A2). Hence,

$$T_{vp} = \overline{T}_{vp} + k(p)(\theta_{ws} - \overline{\theta}_{ws}). \tag{A3}$$

Now taking the sum over a month, we get

$$\sum_{i=1}^{N} T_{vp_i} = N\overline{T}_{vp} + k(p)\sum_{i=1}^{N}(\theta_{ws_i} - \overline{\theta}_{ws}). \tag{A4}$$

Data obtained from a ship cruise in the Bay of Bengal during August–September 1990, which was a convective period (*e.g.*, Seetaramayya *et al.*, 1993), were used to estimate the last summation. The difference between θ_w based on the average temperature and mixing ratio and the mean of daily θ_w is found to be less than 0.04°C for these observations. We assume that the same is true for other observations over tropical oceans. Then the contribution of the second term in (A4) is small and hence can be neglected. Therefore,

$$\sum_{i=1}^{N} T_{vp_i} \cong N\overline{T}_{vp}. \tag{A5}$$

Now, taking the summation of individual CAPE values, we get from Eq. (1)

$$\sum_{i=1}^{N} \mathrm{CAPE}_i = R_d \sum_{i=1}^{N}\int_{\mathrm{LFC}}^{\mathrm{LNB}} (T_{vpi} - T_{vei})d\ln P. \tag{A6}$$

We expect the LFC and LNB to vary depending on the atmospheric conditions. Observations (*e.g.*, Fu *et al.*, 1994, Table 1) show that the changes in LFC and LNB during convective and non-convective periods are small. Further, in general, the variation in CAPE arises mainly due to the variation in the quantity $(T_{vp} - T_{ve})$ and not due to changes in LFC and LNB. Therefore, the summation operator can be taken inside the integral on the right-hand side of (A6). Using (A5), and from the definition of mean $\overline{T}_{ve}$, it follows that

$$\sum_{i=1}^{N} \mathrm{CAPE}_i \cong R_d N \int_{\mathrm{LFC}}^{\mathrm{LNB}} (\overline{T}_{vp} - \overline{T}_{ve})d\ln P \tag{A7}$$

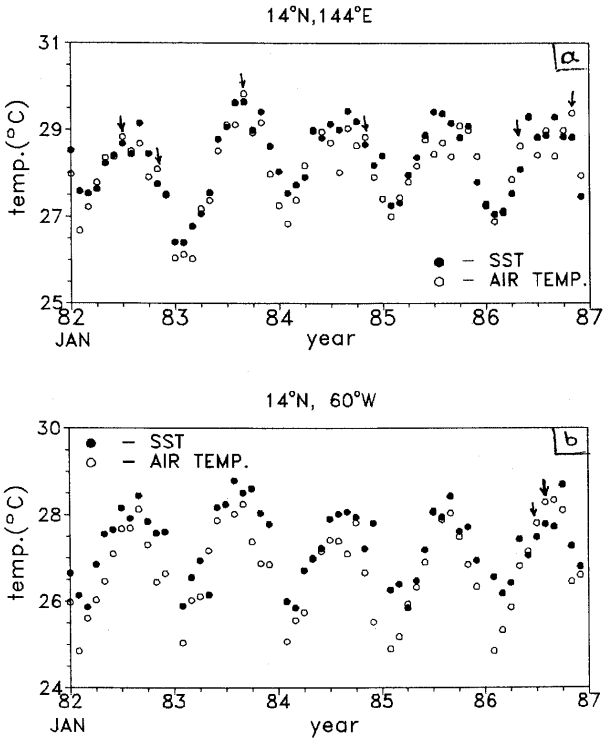

Fig. B1. Surface air temperature and SST from COADS for the period January 82 to December 86. (a) Guam. (b) Grantley.

$$= Nx\mathrm{MCAPE}, \tag{A8}$$

$$\text{or } \mathrm{MCAPE} = 1/N \sum_{i=1}^{N} \mathrm{CAPE}_i. \tag{A9}$$

Hence, MCAPE and the average CAPE based on daily soundings are comparable.

B : *COADS Air Temperature*

Figures B1.a and B1.b show the surface air temperature and SST reported in COADS for the grids where Guam and Grantley are respectively located. There are certain months (some marked by arrow) during which the air is reported to be warmer than the ocean. Over tropical oceans, air temperature may exceed SST over a short time period on any given day (*e.g.*, Malkus, 1964). However, "air warmer than sea" cases are very rare (Roll, 1965, p. 369). Further, a positive air-sea temperature difference suggests a net sensible heat transfer from air to the ocean. Such a possibility over the open oceans (*i.e.*, far from large land masses as in the present case) for the period of a month is not physically possible. Therefore, COADS surface air temperature is not very accurate (at least in these grids), an observation in agreement with the earlier work of Trenberth *et al.* (1992).

C : *Atmospheric Heat Engine*

Computation of large-scale divergence in regions of deep convection (*e.g.*, Frank, 1977) shows that there is convergence near the surface in the lowest 150 mb with a peak around 950 mb and a strong divergence aloft around 200 mb with very weak convergence/divergence in between. In the region of low level convergence, moist air ascends in cumulonimbus clouds and diverges at high levels. The air leaving the deep convective region undergoes radiative cooling, slowly subsides in the clear regions, and returns to the mixed-layer in about 30 days (Emanuel 1994).

In the present study, the model is intended to be simple but representative of the above large-scale circulation pattern. In this spirit, the atmosphere is divided into two régimes, the lowest mixed-layer and a layer above, say the upper layer, that encompasses the rest of the troposphere. The mixed-layer air interacts with the underlying ocean all the time and so its properties are related to the conditions near the surface (*e.g.*, SST, wind speed, subsidence velocity *etc.*, see Betts and Ridgway 1989). Usually, the cloud base is located slightly above the mixed-layer. The upper layer does not interact with the ocean directly, except when deep convective clouds form. A schematic of this circulation pattern is shown in Fig. 7.

Now construct a closed cycle 0-1-2-3-4-0 between the surface and the upper troposphere as shown in Fig. 7. In this cycle, Points 0 and 4 are within the mixed-layer, Points 1 and 3 are just above the mixed-layer, and 2 is in the upper troposphere. For convenience, let us consider an air parcel having unit mass of dry air to be the working fluid in the cycle. Next we like to show that this cycle works like a conventional heat engine.

First, let us understand how a standard automobile engine works. In the present problem, a diesel engine provides a good analogy and therefore this engine is considered for illustration. In a diesel engine, air is drawn into the engine cylinder, it is compressed, fuel is added and the air-fuel mixture burns, and the hot gases expand producing work on the piston. The gases leave through the exhaust valve and fresh air enters through the inlet valve. In the real engine, air (the working fluid) does not follow a closed path. It has been shown that the assumption of an equivalent closed cycle and its analysis provides useful physical insight regarding the performance of the real engine (*e.g.*, Heywood, 1988). An idealized diesel engine cycle can be represented on a pressure — volume diagram as shown in Fig. C1 (Heywood, 1988). In this cycle, air is at atmospheric pressure at Point 1 and is compressed along 1-2, and the work is done by the piston on the air. Path 2-3 corresponds to the fuel injection and its burning in the engine (nearly an isobaric process). Between 3 and 4 air expands further, producing work on the piston. Between 4 and 1, the air is cooled at constant volume to the ambient conditions (exhaust gas

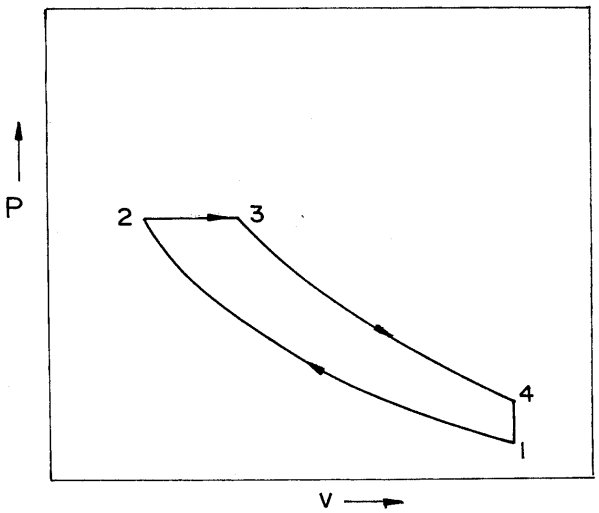

Fig. C1. Ideal diesel (compression-ignition) engine cycle.

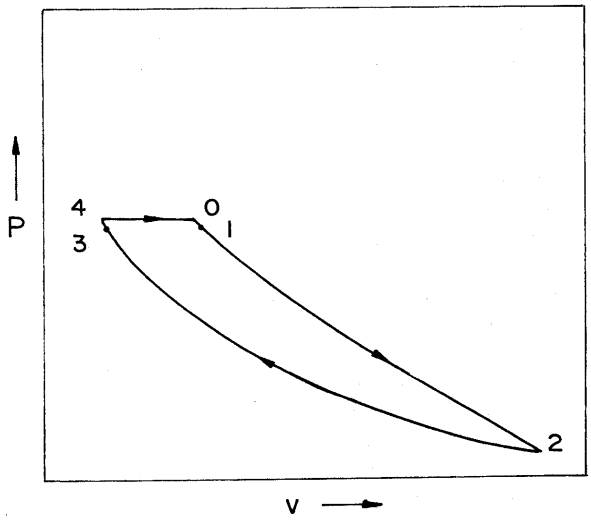

Fig. C2. Schematic representation of the cycle shown in Fig. 7 on a pressure — volume diagram.

discharged into the atmosphere and fresh air taken in, in the real engine). Notice that the expanding air is warmer than the air being compressed at any pressure, and this expansion at warmer temperature and compression and colder temperature leads to net work being produced during a complete cycle.

Now let us see how the cycle shown in Fig. 7 compares with that shown in Fig. C1. The cycle shown in Fig. 7 is schematically given on a pressure-volume diagram in Fig. C2. Along Path 2-3 in Fig. C2 air is compressed and is the analog of the Path 1-2 shown in Fig. C1. Along Path 3-4-0 (Fig. C2) sensible heat and water vapour (here the water vapour is the analog of fuel in an automobile engine) are added to the air, and is the analog of Path 2-3 in the diesel engine cycle (Fig. C1). Along the Path 0-1-2 (Fig. C2) air expands and it does work on the environment, and is the analog of Path 3-4 in Fig. C1. Since there is lot of moisture in the air at point 0, as air expands and cools along 1-2, parcel becomes saturated with respect to water vapour and the amount of water vapour more than that required to keep the parcel just above the saturation level condenses out. In the process, latent heat is released (which enables the ascending parcel to partially overcome the cooling due to expansion and maintain a positive buoyancy), and this is like the fuel being burnt while the air is expanding in an automobile engine (imagine a situation where not all fuel is burnt at Point 3 and part of it being burnt along 3-4 in the diesel engine). By the time the air parcel reaches Point 2 almost all the vapour would have condensed out and air is practically dry, and it is like all fuel being burnt in the engine.

Therefore, there is a close analogy between the cycles shown in Figs. 7 and C1. Hence, the ideal cycle 0-1-2-3-4-0 shown in Fig. 7 can be thought of as representing the atmospheric heat engine. We like to caution the reader that the concept of the atmospheric heat engine exists at a certain level of idealization. In the real atmosphere, mixing of different air masses complicates the matter. However, there is no denying of the fact that there is a broad air flow pattern similar to that shown in Fig. 7 associated with the tropical circulation. Further, air expands and gets compressed at different temperatures at any given pressure.

Now, in an automobile engine the net work realized during the engine's cycle is responsible for its motion and if the net work is not positive and large enough, the engine will stop. In analogy, the work done during the cycle 0-1-2-3-4-0, if positive, can be used for maintaining the large-scale circulation against frictional dissipation. This requires that the expanding air is warmer than the air being compressed at any pressure. As discussed in Section 5, observations support this possibility.

References

Arakawa, A. and W.H. Schubert, 1974: Interaction of a cumulus cloud ensemble with the large-scale environment. *J. Atmos. Sci.*, **31**, 674–701.

Betts, A.K., 1986: A new convective adjustment scheme. Part I: Observational and theoretical basis. *Quart. J. Roy. Meteor. Soc.*, **112**, 677–691.

Betts, A.K. and W. Ridgway, 1989: Climate equilibrium of the atmospheric convective boundary layer over a tropical ocean. *J. Atmos. Sci.*, **46**, 2621–2641.

Bjerknes, J., 1969: Atmospheric teleconnections from the equatorial Pacific. *Mon. Wea. Rev.*, **97**, 163–172.

Bottomley, M., C.K. Folland, J. Hsuing, R.E. Newell and D.E. Parker, 1990: *Global Ocean Surface Temperature Atlas.* U.K. Meteor. Office.

Charney, J.G. and A. Eliassen, 1964: On the growth of the hurricane depression. *J. Atmos. Sci.*, **21**, 68–75.
Ebert, E.F. and G.J. Holland, 1992: Observation of record cloud-top temperatures in tropical cyclone Hilda (1990). *Mon. Wea. Rev.*, **120**, 2240–2251.
Emanuel, K.A., 1994: *Atmospheric Convection.* Oxford University Press, New York.
Emanuel, K.A., J.D. Neelin and C.S. Bretherton, 1994: On large-scale circulations in convecting atmospheres. *Q. J. Roy. Meteor. Soc.*, **120**, 1111–1143.
Frank, W.M., 1977: The structure and energetics of the tropical cyclone I. Storm structure. *Mon. Wea. Rev.*, **105**, 1119–1135.
Fu, R., A.D. Del Genio and W.B. Rossow, 1994: Influence of ocean surface conditions on atmospheric vertical thermodynamic structure and deep convection. *J. Climate*, **7**, 1092–1108.
Gadgil, S., P.V. Joseph and N.V. Joshi, 1984: Ocean-atmosphere coupling over monsoonal regions. *Nature*, **312**, 141–143.
Garcia, O., 1985: *Atlas of Highly Reflective Clouds for the Global Tropics: 1971–1983.* U.S. Department of Commerce, NOAA, Environmental Research Laboratory.
Graham, N.E. and T.P. Barnett, 1987: Sea surface temperature, surface wind divergence, and convection over tropical oceans. *Science*, **238**, 657–659.
Heywood, J.B., 1988: *Internal combustion engine fundamentals*, McGraw-Hill.
Lau, K.M. and S. Shen, 1988: On the dynamics of intraseasonal oscillations and ENSO. *J. Atmos. Sci.*, **45**, 1781–1797.
LeMone, M.A., 1980: The marine boundary layer. In J.G. Wyngaard (ed.) *Workshop on the Planetary Boundary Layer*, 14–18 August 1978, Boulder, Colorado, American Meteorological Society, pp. 182–231.
Malkus, J.S., 1964: Tropical convection: progress and outlook. In *Proc. of the WMO IUGG Symposium on Tropical Meteorology, 5–13 Nov.*, 1963, Rotorua, New Zealand, pp. 247–277.
Moncrief, M.W. and M.J. Miller, 1976: The dynamics and simulation of tropical cumulonimbus and squall lines. *Q. J. Roy. Meteor. Soc.*, **102**, 373–394.
Neelin, J.D. and I.M. Held, 1987: Modelling tropical convergence based on moist static energy budget. *Mon. Wea. Rev.*, **115**, 3–12.
Palmen, E., 1948: On the formation and structure of tropical hurricanes. *Geophysica* (Helsinki) **3**, 26–38.
Paluch, I.R., 1979: The entrainment mechanism in Colorado cumuli. *J. Atmos. Sci.*, **36**, 2467–2478.
Raymond, D.J., 1994: Convective processes and tropical atmospheric circulations. *Q. J. Roy. Meteor. Soc.*, **120**, 1431–1455.
Roll, H.U., 1965: *Physics of the Marine Atmosphere.* Academic Press.
Saunders, P.M., 1957: The thermodynamics of saturated air: a contribution to the classical theory. *Q. J. Roy. Meteor. Soc.*, **83**, 342–350.
Seetaramayya, P., S.S. Parasnis, S.G. Nagar and K.G. Vernekar, 1993: Thermodynamic structure of the boundary layer in relation to a monsoon depression over the Bay of Bengal — A case study. *Boundary-Layer Meteor.*, **65**, 307–314.
Slutz, R.J., S.J. Lubker, J.D. Hiscox, S.D. Woodruff, R.L. Jenne, D.H. Joseph, P.M. Steurer and J.D. Elms, 1985: *COADS: Comprehensive Ocean-Atmosphere Data Set.* Release 1, 262 pp.
Trenberth, K.E., J.R. Christy and J.W. Hurrel, 1992: Monitoring global monthly mean surface temperatures. *J. Climate*, **5**, 1405–1423.
Waliser, D.A., N.E. Graham and C. Gautier, 1993: Comparison of the highly reflective cloud and outgoing longwave radiation datasets for use in estimating tropical deep convection. *J. Climate*, **6**, 331–353.
Williams, E.R. and N. Renno, 1993: An analysis of the conditional instability of the tropical atmosphere. *Mon. Wea. Rev.*, **121**, 21–35.
Williams, E.R., S.A. Rutledge, S.G. Geotis, N. Renno, E. Rasmussen and T. Rickenbach, 1992: A radar and electrical study of tropical "Hot Towers". *J. Atmos. Sci.*, **49**, 1386–1395.
Xu, K. and K.A. Emanuel, 1989: Is the tropical atmosphere conditionally unstable? *Mon. Wea. Rev.*, **117**, 1471–1479.
Zhang, C., 1993: Large-scale variability of atmospheric deep convection in relation to sea surface temperature in the tropics. *J. Climate*, **6**, 1898–1913.

熱帯対流活動、対流有効位置エネルギーと海面水温

G.S. Bhat・J. Srinivasan and Sulochana Gadgil
（インド理学研究所大気科学センター）

高層気象観測の月平均値に基づいて、対流有効位置エネルギー (convective available potential energy; CAPE) を熱帯対流活動と関連づけて評価した。

熱帯大西洋と西部太平洋の観測点の解析から、海面水温と共にCAPEの変動は活発な対流活動の頻度の変動に類似していることがわかった。これは、熱帯対流活動の頻度とCAPEとの強い関連性を示唆する。CAPEは、対流域での上昇、その周辺の晴天域での下降を伴った、境界層上の仕事ポテンシャルとして理解できることを示した。